Aalto University
School of Electrical Engineering
Department of Micro and Nanosciences
Master's Programme in Micro and Nanotechnology

Jie Su

Optimization of TiO_2 Thin Film Growth at Different Temperatures by Atomic Layer Deposition

Master's thesis submitted in partial fulfillment of the requirements for the degree of Master of Science in Technology.

Espoo, Finland, 11th 11, 2011

Supervisor: Prof. Harri Lipsanen

Instructor: Doc. Teppo Huhtio
MSc. Markus Bosund

ACKNOWLEDGEMENTS

The thesis was carried out in the Nanotechnology Group of the Department of Micro and Nanosciences of Aalto University School of Electrical Engineering. The work is part of the project "*Novel nanofabrication methods for specialty optical fibers*" funded by the Finnish Funding Agency for Technology and Innovation (TEKES).

First and foremost, I would like to show my deepest gratitude to Prof. Harri Lipsanen and Docent Teppo Huhtio for giving me an opportunity to work in their group as well as their supervision in my work. I appreciate the valuable guidance in every stage of the writing of this thesis by Docent Teppo Huhtio with his kindness and patience. I would like to thank Mr. Markus Bosund for his instructions and suggestions in the work. My sincere appreciation also goes to all my teachers during my study in Finland.

I shall extend my thanks to all my friends, especially Yang Liu, Ying Wu, Hao Zhang, Shuo Li, Zhen Zhu and Yanfeng Li, for their encouragement and support during my thesis work.

Last but not least, I owe special thanks to my father (Mr. Shenghua Su), my mother (Mrs. Meihua Chen) and my boyfriend (Ling Luo) for their concern and great encouragement for the years.

Otaniemi, 11. 11. 2011

Jie Su

Aalto University
School of Electrical Engineering
Master's Programme in Micro and Nanotechnology

ABSTRACT OF MASTER'S THESIS

Author: Jie Su

Title of Thesis: Optimization of TiO_2 Thin Film Growth at Different Temperatures by Atomic Layer Deposition

Date: 11/ 11/ 2011 Pages: iv+52

Department: Micro and Nanosciences

Professorship: Nanotechnology Code: S - 104

Supervisor: Prof. Harri Lipsanen

Instructor: Docent Teppo Huhtio
M. Sc. Markus Bosund

In this work TiO_2 films were grown on silicon substrates by atomic layer deposition (ALD) using $TiCl_4$ and H_2O as precursors. The effect of precursor pulse length and reaction temperature on the film growth rate and film uniformity was studied. The film thickness and refractive indices were measured by ellipsometry.

The simulation of TiO_2 growth with different $TiCl_4$ pulsing lengths was carried out. The results indicated that in an appropriate temperature range the growth rate and the uniformity are insensitive to a longer pulsing length.

In the temperature optimization experiment, TiO_2 films with a small thickness variation of 1% - 4% and growth rate (0.4 Å - 0.5 Å/cycle) were obtained in the temperature range of 200 °C to 300 °C.

Keywords: atomic layer deposition, titanium oxide, $TiCl_4$, temperature, precursor pulsing, growth rate, uniformity, thickness variation

TABLE OF CONTENTS

1. INTRODUCTION..1

2. THEORY OF ATOMIC LAYER DEPOSITION 4

2.1 Principles of ALD 4

2.2 Effects of ALD growth parameters on thin films...6

2.2.1 Effects of growth temperature 6

2.2.2 Effects of number of cycles 8

2.2.3. Effects of precursor pulse length 10

2.2.4. Effects of purge length..11

2.3 ALD precursors 11

2.4 Growth chemistry of TiO_2...12

3. THEORY OF ELLIPSOMETRY 15

3.1 Polarization of light..15

3.2 Principles of spectroscopic ellipsometry..18

3.3 Uniformity measurement 19

4. EXPERIMENTAL TECHNIQUES AND MOTHODS................................21

4.1 ALD equipment..21

4.2 Ellipsometer 23

4.3 Preparation of substrates before ALD 26

4.4 Optimization of parameters 27

5. RESULTS AND DISCUSSION 29

5.1 $TiCl_4$ pulse length optimization 30

5.2 Growth linearity 35

5.2.1 Thickness and growth linearity 35

5.2.2 Growth rate versus number of cycles 36

5.3 Optimization of temperature 37

5.3.1 Temperature dependence of growth rate 38

5.3.2 Temperature dependence of uniformity 40

5.4 Optical characterization of TiO_2 films 44

6. CONCLUSIONS 47

REFERENCES 49

Chapter 1

Introduction

Titanium dioxide thin films are extensively used due to their attractive physical, chemical and optoelectronic properties. TiO_2 thin films have good transmittance in the visible region, high refractive index, high dielectric constant, high catalytic activity and chemical stability.[1] A great deal of research has been directed at their use in applications involving high refractive index optical coatings,[2] photocatalytic coatings for air and water purification, self-cleaning surfaces and sterilization,[3,4] biocompatible coatings,[5] corrosion protection coatings,[6] high permittivity dielectric layers for electronic devices[7] and photochemical solar cells.[8]

Due to the great interest, the preparation methods of TiO_2 thin films have been studied and innovated. A variety of deposition techniques have been used such as sol-gel processes,[9] chemical vapor deposition (CVD),[10 11] electron beam evaporation,[12] various sputtering depositions,[13 14] ion beam-assisted processes[15] and atomic layer deposition (ALD).[16] However, most of the photocatalytic TiO_2 thin films used in the market are prepared by low-cost wet processes such as the sol-gel method. Although the films show excellent photocatalytic activity, the mechanical durability is not good enough for practical uses. In addition, the uniformity of the thickness in a large area is poor. Furthermore, the thin film

thickness cannot be controlled accurately. The disadvantages cause limitations in applications which require quite thin films with uniform thickness on large-area substrates.

Compared with other deposition techniques, ALD distinguishes itself with its superiorities. ALD was introduced world widely in the 1970s by Tuomo Suntola and his co-workers with a name of atomic layer epitaxy (ALE). It is a chemical vapor thin film deposition method based on self-limiting alternate saturated surface reactions. As distinct from the other chemical vapor deposition techniques, in ALD the source vapors are pulsed into the reactor alternately, once at a time, separated by purging or evacuation periods. Each precursor exposure step saturates the surface with a monomolecular layer of that precursor. This results in a unique self-limiting film growth mechanism with a number of advantageous features, such as excellent conformability and uniformity, and simple and accurate film thickness control. The requirement of high dielectric strength and good uniformity over large-area or non-flat substrates can be met by ALD successfully.

The uniformity of a thin film in an ideal ALD process is excellent. Nevertheless, in real processes some technical issues such as reacting temperature, precursor exposure time (pulse length), purging length and substrate surface contamination can affect thickness uniformity. At different temperatures ALD layer growth presents dissimilar uniformity. Longer exposure time may lead to decomposition of the precursor while long purging length may result in desorption of chemisorbed precursor molecules.

In this work the effect of growth temperature and precursor pulse length on the uniformity of TiO_2 thin films is studied. Because of the effect of temperature, there should be a temperature range around which the film growth results in better

uniformity. The goal of this work is to: 1) model and simulate the influence of growth temperature and precursor pulse length in the TiO_2 ALD growth process, and 2) to optimize the growth temperature the precursor pulse length in the TiO_2 ALD growth process. In this work the uniformity of TiO_2 films grown at different temperatures and with different precursor pulse lengths is measured and studied. TiO_2 films were grown by ALD on silicon substrates using the precursors of titanium tetrachloride ($TiCl_4$) and water (H_2O) at different growth temperatures ranging from 100 °C to 450 °C. Thin film thicknesses and uniformities were measured by ellipsometry. The work was carried out in the Department of Micro and Nanosciences using the cleanroom and other facilities at Micronova Research Centre.

The thesis is constituted as follows: a general introduction is given in chapter one. In the second chapter, theory of ALD is introduced. Theory of ellipsometry is presented in chapter three, followed by a description of experimental techniques and methods in chapter four. In chapter five, the results of the experiment and measurement are analyzed and discussed. A conclusion of the work is given in the last chapter.

Chapter 2

Theory of Atomic Layer Deposition

In this chapter an overview of the working principles of ALD and the effects of ALD growth parameters on thin films are given. Precursor chemistry of ALD as well as the growth chemistry of TiO_2 is provided.

2.1 Principles of ALD

ALD is based on sequential self-terminating gas-solid reactions. Alternating pulses of two precursors, separated by a purge of inert gas, constitute a typical ALD cycle. The cycle consists of the following four steps illustrated in ***Fig. 1***: [17]

(i) A first pulsing step: exposure of the first reactant (precursor A) and a self-terminating chemisorption of precursor A on the surface.

(ii) An inert gas purge or evacuation to remove the non-reacted reactants and the gaseous reaction by-products.

(iii) A second pulsing step: exposure of the second reactant (precursor B) and a self-terminating reaction of precursor B - or another treatment to activate the surface again for the reaction of the first reactant.

(iv) An inert gas purge or evacuation.

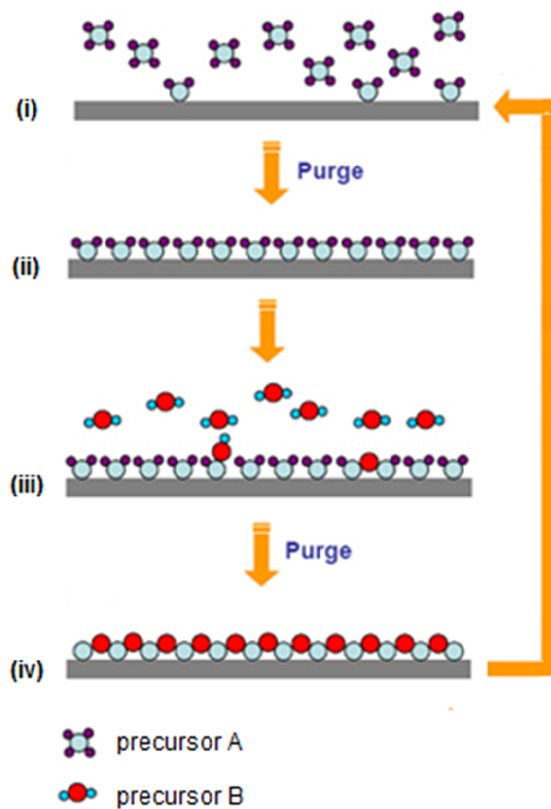

Fig. 1. *Schematic illustration of an ALD reaction cycle.*[18]

The actual reactions taking place under each exposure step depend largely on the presence or the absence of precursors on the surface of the growing film. First a finite number of the reactions or chemisorption of precursor A occur on the surface, in maximum only a monomolecular layer of the precursor is chemisorbed on the surface. The following purging period removes all the excess precursor molecules and byproducts leaving only the monolayer on the surface. Afterwards reactant B is dosed in and reacts with the chemisorption layer producing the desired film. The second purging period completes the deposition cycle which is then repeated as many times as required for the desired film thickness.[17] The reactions are driven to completion in each cycle so that reaction cites are all occupied by the precursor molecules or the desired thin film.

The thin film growth is self-limiting in ALD. Ideally, each exposure and purging step is complete. Precursor A and precursor B are chemisorbed or react completely and the purging step removes all the excess molecules and byproducts. The amount of the desired thin film deposited during each cycle is the same and is only determined by the density of the chemisorption or reaction sites at the surface.

One of the advantages of ALD is the precise thickness control at atomic layer level. It is able to meet the needs of excellent step coverage and conformal coating on high aspect ratio structures. The self-limiting feature of the surface reaction results in smooth and continuous films, which is another superiority of ALD. ALD is also extendible to three-dimension coating and parallel processing of batch substrates. In addition, high reaction activity of precursors gives possibility to low temperature (below 400 °C) growth. The main disadvantage, however, is the low deposition rate since usually a fraction of a monolayer is deposited in one cycle.

2.2 Effects of ALD growth parameters on thin films

Film growth rate and film properties, e.g. uniformity and surface morphology, are the elements to assess the quality of a thin film. To find the best condition for high quality thin films, the effects of growth temperatures, number of cycles, precursor pulse length, precursor fluxes and purge length should be taken into account.

2.2.1 Effects of growth temperature

The surface morphology of an ALD-grown film is sensitive to the reaction temperature in the film growth. A concept of 'ALD-window', first introduced by Suntola et al.,[19] indicates the temperature range where thin film growth proceeds in an ALD-mode. Different kinds of growth rate versus temperature dependencies are schematically illustrated in ***Fig. 2***.

(i) It is expected that the growth proceeds in the self-limiting manner and with a temperature independent rate in the middle of the temperature range (acceptable window).[20] In this situation, steric hindrance causes saturation and the number of reactive sites does not affect the amount of adsorbed species.[21] Although in real case many precursors do not exhibit a distinct ALD window and thus the deposition rate in these processes is dependent on the temperature, they can still be used for self-limiting ALD processes.[22]

(ii) In the low temperature side of the self-limiting region, the growth rate decreases with increasing temperature. If the surface density of the chemisorbed species is temperature dependent, the growth rate usually decreases with increasing temperature because of a decreased density of reactive –OH groups on the surface. It may occur due to a multilayer adsorption and the condensation of low vapor pressure precursors at low temperature.[16]

(iii) In the low temperature side of the self-limiting region, the growth rate decreases with decreasing temperature. The decrease may be related to kinetic reasons; i.e., the growth reactions become so slow that they are not completed within the given pulse length.

(iv) At high temperature the precursor may decompose and be adsorbed on the substrate surface, resulting in the increase of the growth rate. Besides, an increase

of the growth rate may occur when some energy barriers are overcome and reactions which do not happen at lower temperatures take place.[23]

(v) Decrease of the growth rate in the high temperature side of the self-limiting region is related to a desorption of the precursors[16] or precursor re-evaporation.[24]

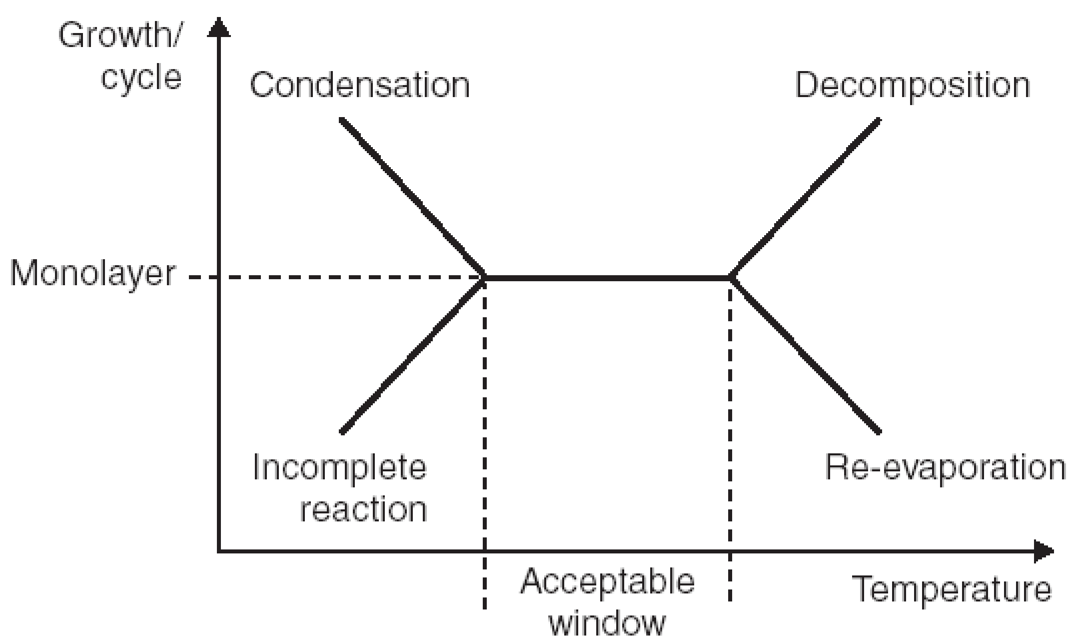

Fig. 2. *Dependency of the growth rate on temperature in ALD.*[16]

2.2.2 Effects of number of cycles

In the ALD process, the chemical composition of the surface is changed compared to the original surface. The growth rate per cycle should be varied if the chemical composition of the surface is changed. The first reaction cycle takes place on the original surface of the substrate, with the following reaction on a surface with both the original surface and the material deposited by the first cycle. After several cycles, the substrate surface is covered by ALD-grown material with no

original surface exposed. After a sufficient number of cycles, the growth rate per cycle is expected to settle to a constant value. The way how the growth rate per cycle varies with the number of cycles can be used as a means to divide the ALD processes in four groups.

The classification is summarized in ***Fig. 3***.[25] In linear growth, the growth rate per cycle can be constant over the cycles [***Fig. 3****(a)*]. In substrate-enhanced growth, the growth rate per cycle can be higher in the beginning of the growth than at the steady region and then increase to the steady value [***Fig. 3****(b)*]. In substrate-inhibited growth, the initial growth rate per cycle can be lower due to less reactive sites on substrate than on grown layer. In substrate-inhibited growth type 1, the growth rate per cycle can be lower in the beginning of the growth than at the steady region and then increase to the steady value [***Fig. 3****(c)*] while in type 2 the growth rate per cycle increases gradually to a peak and then decreases to the steady value [***Fig. 3****(d)*].[25]

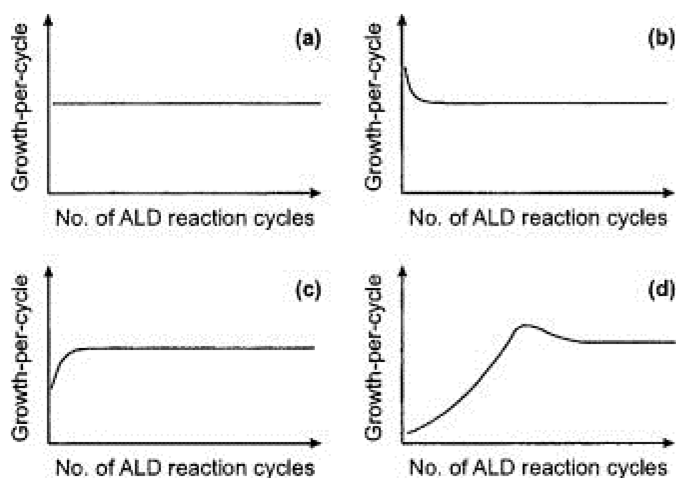

Fig. 3. *Classification for the ALD processes: (a) linear growth, (b) substrate-enhanced growth, (c) substrate-inhibited growth of type 1, and (d) substrate-inhibited growth of type 2.*[25]

2.2.3. Effects of precursor pulse length

When keeping the carrier gas flow rate, the precursor temperature and the reactor pressure as constants, precursor pulse length will be the main parameter affecting the amount of precursor arriving on the substrate in every ALD cycle. If the pulse length is so short that not enough precursor molecules are transported to the reaction chamber, there will not be enough precursor molecules for all of the active sites and the growth cannot reach to a saturated level.

In an ideal case, the reactions are fast and the saturation level is rapidly achieved (***Fig. 4*** *a*). The saturation level can be reached gradually if the precursors are less reactive (***Fig. 4*** *b*). Overlong pulse length can cause the change of growth rate. If the precursor is decomposing thermally, the growth rate per cycle will increase with pulsing length (***Fig. 4*** *c*). Etching reactions may take place resulting in a decrease of the growth rate per cycle (***Fig. 4*** *d*).

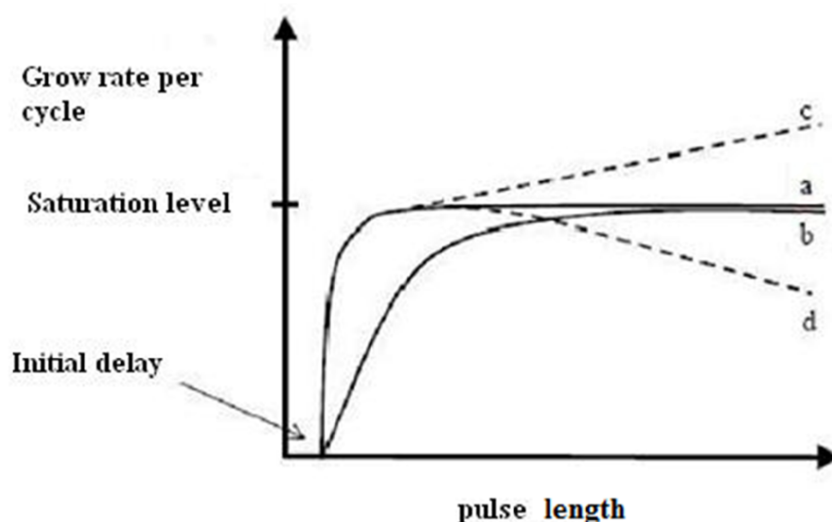

Fig. 4. *Behavior of the growth rate as a function of pulse length in ALD.*[16]

2.2.4. Effects of purge length

Purging is used in ALD growth in order to avoid overlapping of precursor pulses and to purge away the by-products produced by the reactions. Due to an insufficient purging length excess precursors remain on the substrate, causing chemical vapor deposition and resulting in a fast growth rate and film non-uniformity. If corrosive by-products are remained on the substrate, etching of the substrate will take place resulting in a decrease of the growth rate. Therefore, a sufficient purge length is necessary for the self-limiting growth. For a given reactor, an appropriate purge length can be used in different processes as the purge length is reactor dependent but not so much dependent on the precursors.[16] The purge length does not have to be changed provided that it is optimized for a given reactor.

2.3 ALD precursors

In a successful ALD process, choice of the precursors is the main issue. The desired properties of ALD precursors should be examined in the process design. In general there are some basic requirements for the precursors.[16]

(i) High reaction activity and aggressive to ensure the fast reaction completion.

(ii) Excellent volatility at the source temperature.

(iii) Remarkable thermal stability.

(iv) No dissolution into the substrate or the film.

(v) High purity.

(vi) Low cost and environment-friendliness.

Metal halides, metal alkoxides and H_2O, H_2O_2, NH_3 are extensively used as

precursors in ALD as they have eligible chemical properties to meet the demanding requirements.

2.4 Growth chemistry of TiO2

Different precursors have been examined and used in ALD of TiO_2 in recent years. Titanium alkoxides like titanium-isopropoxide ($Ti\{OCH(CH_3)_2\}_4$), titanium-ethoxide ($Ti(CH_3CH_2O)_4$), and titanium-methoxide ($Ti\{(CH_3)O\}_4$)[26,27,28] as well as tetrakis (dimethylamido) titanium (TDMAT)[29] were used as metal precursor for TiO_2 thin film research. The most widely investigated precursor is titanium tetrachloride ($TiCl_4$) with water (H_2O).

In this work $TiCl_4$ and H_2O are used as precursors. The reaction between these reactants can be described as:

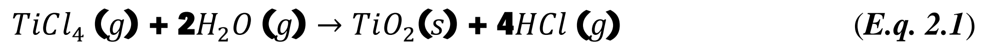

$$TiCl_4\ (g) + 2H_2O\ (g) \rightarrow TiO_2(s) + 4HCl\ (g) \qquad (\textit{E.q. 2.1})$$

There are two hypothetical routes in the TiO_2 ALD process depending on the presence or absence of hydroxyl group on the substrate surface (***Fig. 5*** and ***Fig. 6***).

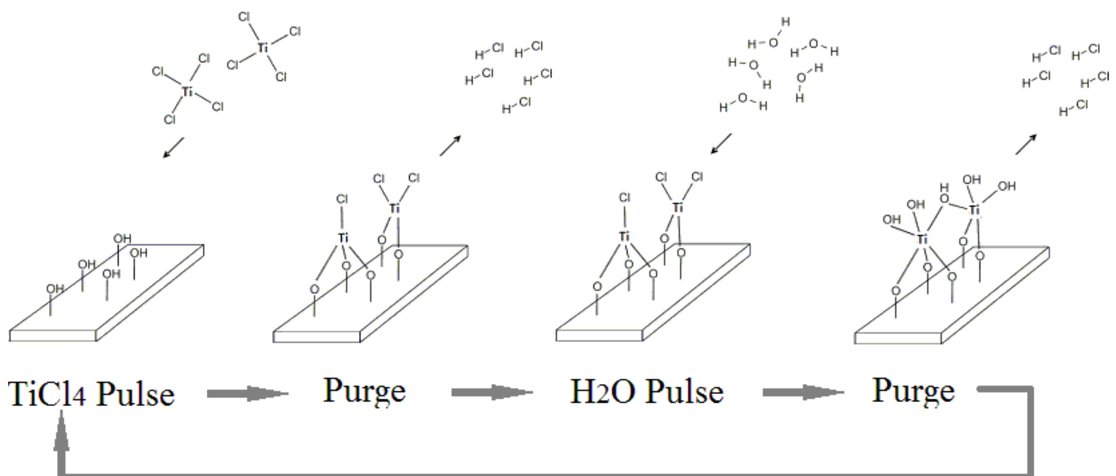

Fig. 5. *A TiO_2 film ALD process shown schematically on a hydroxyl terminated*

surface.

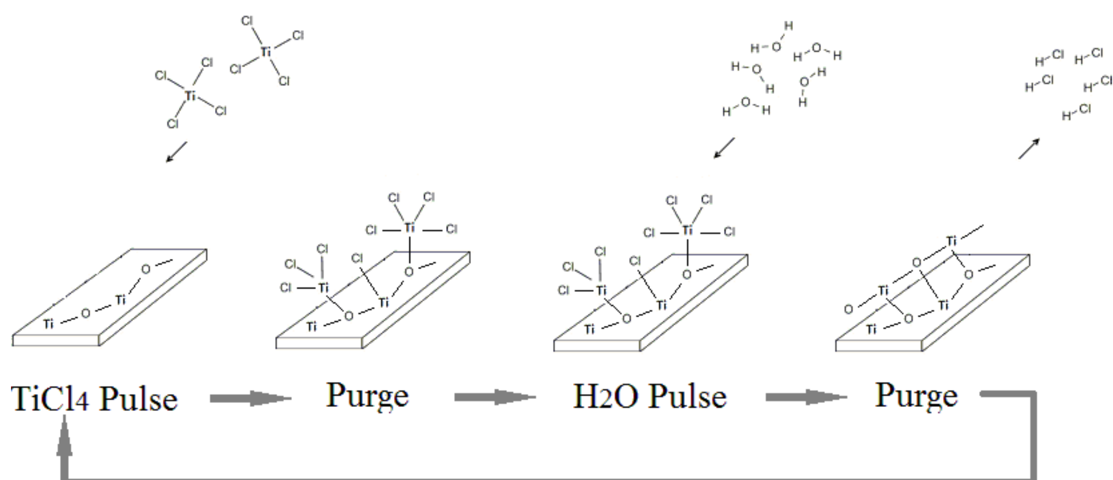

Fig. 6. *A TiO_2 film ALD process shown schematically on a dehydroxylated surface.*

On an –OH group terminated surface, $TiCl_4$ is pulsed and reacts with these hydroxyl groups releasing some of the Cl^- ligands (***E.q. 2.2***), while on a completely dehydroxylated surface, $TiCl_4$ is pulsed and chemisorbs on the surface. After the first purging step, the excess precursor of $TiCl_4$ and HCl in gas phase is purged away. $TiCl_x$ species (x may be 0, 1, 2, 3 or 4) are attached to the surface. Only a monolayer of the $TiCl_x$ species can be attached to the surface per reaction or chemisorption. In the H_2O pulsing step, H_2O reaction removes the chloride ligands from the surface as HCl and leaves behind a TiO_2 surface. Subsequently, the surface is either –OH terminated or TiO_2 covered. The whole cycle is completed with a second purge and the next cycle is then repeated. Oxygen bridges can also form during the reaction of H_2O, as two –OH groups can release H_2O and form an oxygen bridge, which is called dehydroxylation (***E.q. 2.3***). The –OH group content will settle to a temperature-dependent value in the H_2O reaction.[30]

$$x(-OH) + TiCl_4(g) \longrightarrow (-O-)_x TiCl_{4-x} + xHCl(g) \qquad (\textbf{E.q. 2.2})$$

$$2(-OH) \rightarrow (-O-) + H_2O \qquad (\textbf{\textit{E.q. 2.3}})$$

Chlorine effect should be taken into consideration when HCl is released after the pulse of $TiCl_4$. HCl may react with the hydroxyl groups and oxygen bridges. (***E.q. 2.4, 2.5, 2.6***)

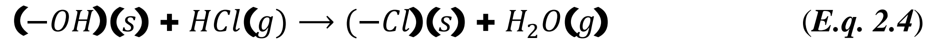

$$(-OH)(s) + HCl(g) \longrightarrow (-Cl)(s) + H_2O(g) \qquad (\textbf{\textit{E.q. 2.4}})$$

$$(-O-)(s) + 2HCl(g) \longrightarrow 2(-Cl)(s) + H_2O(g) \qquad (\textbf{\textit{E.q.2.5}})$$

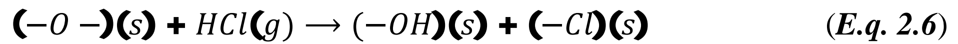

$$(-O-)(s) + HCl(g) \longrightarrow (-OH)(s) + (-Cl)(s) \qquad (\textbf{\textit{E.q. 2.6}})$$

Therefore, the adsorption sites can be occupied by $TiCl_4$, HCl or Cl^-. Steric hindrance must be taken into consideration owing to the larger size of Cl^- than the other ions in the reaction. The adsorption sites may be limited by the high concentration of Cl^- ions.

Chapter 3

Theory of ellipsometry

Ellipsometry is an extensively used optical measurement technique which measures the change of polarization in light reflection and transmission from a material. The change of polarization is associated with the optical properties and thickness of the material. Thus ellipsometry can be used to determine the film thickness and characterize the optical constants as well as the roughness and other material properties related to a change in polarization of light.

3.1 Polarization of light

A light wave with specific oriented electric fields is called polarized light. Light waves (or electromagnetic waves) are three-dimensional transverse waves. If the oscillating direction of light waves is completely random, the light is called unpolarized light. When light waves propagate in the same direction, the polarization is expressed by superimposing each electric field.

We can express the electromagnetic wave traveling along the z axis as the vector sum of the electric fields E_x and E_y (***E.q. 3.1***) [31]

$$\begin{aligned} E(z,t) &= E_x(z,t) + E_y(z,t) \\ &= \left\{ E_{x0} \exp\left[i\left(\omega t - Kz + \delta_x \right) \right] \right\} x + \left\{ E_{y0} \exp\left[i\left(\omega t - Kz + \delta_y \right) \right] \right\} y \end{aligned} \qquad \textbf{(\textit{E.q. 3.1})}$$

where x and y are unit vectors along the coordinate axes, ω is angular frequency, K is the wave number, which equals to $\frac{2\pi}{\lambda}$ showing the number of sinusoidal waves present in the distance from 0 to 2π. With different phase differences $\delta_x - \delta_y$ (or $\delta_y - \delta_x$), light waves represent different kinds of polarization. If $E_{x0} = E_{y0}$ and $K = 1$ are assumed, and when $\delta_x - \delta_y = 7\pi/4$ or $\delta_x - \delta_y = 5\pi/4$, light waves represent clockwise elliptical polarization (***Fig. 7** and **Fig. 8***).

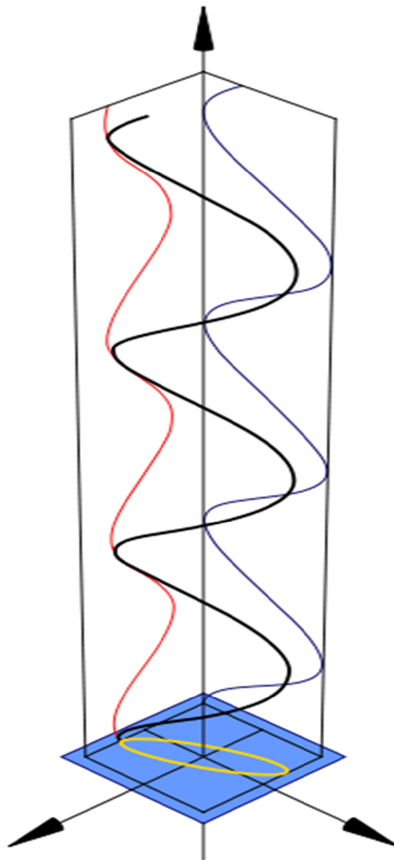

***Fig. 7.** Schematic of elliptical polarized light.*[32]

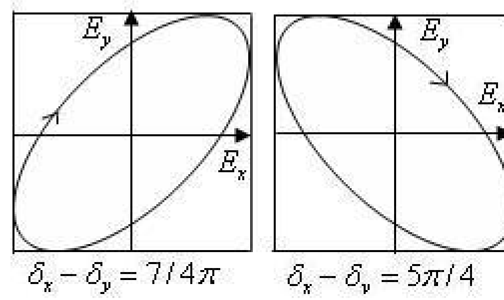

Fig. 8. *Clockwise elliptical polarized light.*[31]

Another frequently used coordinate system of a polarized light is associated with the plane of incidence. Light with an electric field parallel to the plane of incidence is termed as *p*-polarized light, while light with an electric field perpendicular to the plane of incidence is termed as *s*-polarized light (***Fig. 9***).

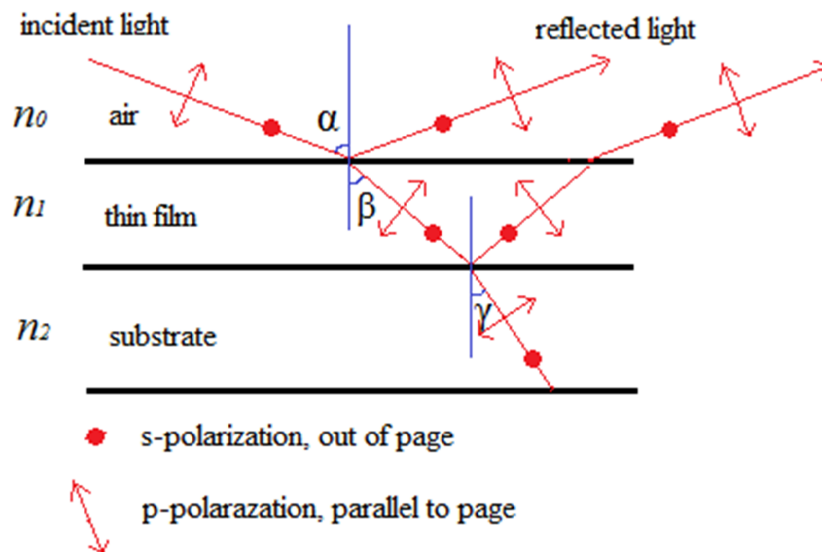

Fig. 9. *s- and p-polarization of light.*

3.2 Principles of spectroscopic ellipsometry

In Ellipsometry, *p*- and *s*-polarized light waves are irradiated onto a sample, and the optical constants and film thickness of the sample are measured from the change in the polarization state by light reflection or transmission. The amplitude reflection coefficients for *p*- and *s*-polarizations differ significantly due to the difference in electric dipole radiation. Ellipsometry measures the two values (ψ, Δ) that express the amplitude ratio and phase difference between *p*- and *s*-polarizations, respectively.[31]

The measured (ψ, Δ) from ellipsometry are defined from the ratio of the amplitude reflection coefficients for *p*- and *s*-polarizations:

$$\rho = \tan\psi \exp(i\Delta) = \frac{r_p}{r_s} = \frac{t_p}{t_s} \qquad (E.q.\ 3.2)$$

where r_p, r_s, t_p and t_s are the amplitude reflection coefficients and transmission coefficients for *p*- and *s*-polarizations, respectively.

Snell's Law gives a relationship between the incident and refractive angles:

$$n_0 \sin\alpha = n_1 \sin\beta = n_2 \sin\gamma \qquad (E.q.\ 3.3)$$

where α is the incident angle, β and γ are the transmission angles. n_0, n_1 and n_2 are the refractive indices of air, thin film and substrate, respectively.

P- and *s*-polarized electric fields are independent and can be calculated separately. The ratio of the amplitude reflection coefficients for *p*- and *s*-polarizations can be described by Fresnel's equations:

$$r_s = \left(\frac{E_{0r}}{E_{0i}}\right)_s = \frac{n_1 \cos\alpha - n_2 \cos\beta}{n_1 \cos\alpha + n_2 \cos\beta} \qquad (E.q.\ 3.4)$$

$$r_p = \left(\frac{E_{0r}}{E_{0i}}\right)_p = \frac{n_2 \cos\alpha - n_1 \cos\beta}{n_2 \cos\alpha + n_1 \cos\beta} \quad \textbf{\textit{(E.q. 3.5)}}$$

$$t_s = \left(\frac{E_{0t}}{E_{0i}}\right)_s = \frac{2n_1 \cos\alpha}{n_1 \cos\alpha + n_2 \cos\beta} \quad \textbf{\textit{(E.q. 3.6)}}$$

$$t_p = \left(\frac{E_{0t}}{E_{0i}}\right)_p = \frac{2n_1 \cos\alpha}{n_1 \cos\beta + n_2 \cos\alpha} \quad \textbf{\textit{(E.q. 3.7)}}$$

Thus the film thickness can be defined as:[33]

$$d = \frac{n_1 \lambda}{2\cos\beta} \quad \textbf{\textit{(E.q. 3.8)}}$$

where λ is the wavelength of incident light.

When a sample structure is simple, the amplitude ratio ψ is characterized by the refractive index *n*, while Δ represents light absorption described by the extinction coefficient *k*. Therefore the two values (n, k) can be determined directly from the two ellipsometry parameters (ψ, Δ) obtained from the measurement.[31]

3.3 Uniformity measurement

To measure the uniformity quantitatively, an ellipsometer is used to measure the thickness and thickness variation of a sample. For each sample, the thicknesses of 10 points on the surface are measured by an ellipsometer and a mean thickness of a sample can be calculated. This is defined as a measurement circle.

Standard deviation of the thickness is one of the scientific measures of the surface variability or uniformity of a film, which is defined by:

$$\delta = \sqrt{\frac{\sum_{i=1}^{N}\left(x_i - \overline{x}\right)^2}{N}} \quad \textbf{\textit{(E.q. 3.9)}}$$

where N is the number of points measured in each measurement circle, x_i is the

thickness measured on each point, and $\bar{x}$ is the average thickness. The value of δ can be read from the ellipsometer.

Chapter 4

Experimental techniques and methods

4.1 ALD equipment

ALD reactors can be divided into two groups: inert gas flow reactors operating under viscous or transition flow conditions at pressures higher than about 1 torr, and high or ultrahigh-vacuum reactors operating under molecular flow conditions.[34]

The main parts of an ALD reactor are:

(i) reaction chamber (***Fig. 10***)

(ii) sources of one or several of the following types: gas, liquid, and solid sources

(iii) flow and sequencing control of the sources

(iv) transport gas supply

(v) temperature control of the heated sources, reaction chamber and the substrate

(vi) vacuum pump and related exhaust equipment

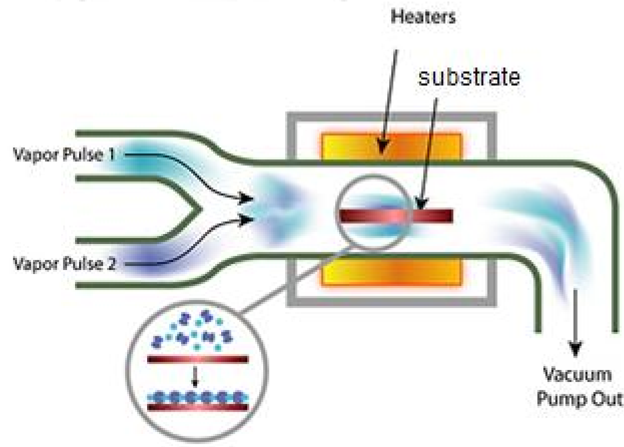

Fig. 10. *Schematic of the reaction chamber of a small-batch ALD reactor.*[35]

In this work a TFS 500 ALD reactor manufactured by BENEQ is used. Below are some characteristics (***Table 1***) and a photograph (***Fig. 11***) of the reactor.

Table 1*. Characteristics of a TFS 500 ALD reactor.*[36]

Reaction chamber	200 mm (diameter) 3 mm (height)
Gas lines	Up to 5
Liquid source	Up to 4
Deposition temperature	25 °C to 500 °C
Length	1600 mm
Width	900 mm
Height	1930 mm
Weight	700 Kg
.Connection power	10 kW
Control system	PLC control + PC user interface

Fig. 11. *A photograph of a TFS 500 ALD reactor.*[37]

4.2 Ellipsometer

As the uniformity of a thin film layer is what we are interested in, one of the key parameters is the thickness of the layer. An ellipsometer is an excellent device for measuring the thickness of extremely thin films (***Fig. 12***).[38]

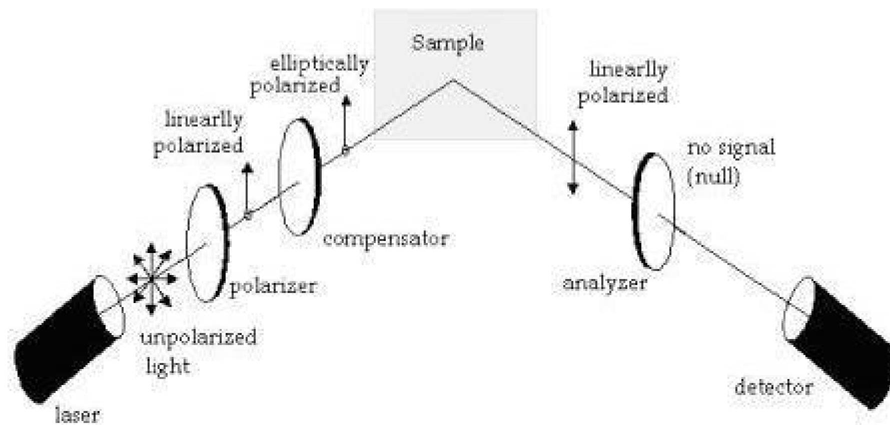

Fig. 12. *A schematic of a polarizer-compensator-sample-analyzer ellipsometer.*[38]

Ellipsometers work by shining a well-defined source of light on a material and capturing the reflection. Ellipsometers measure the changes in the state of polarization of light upon reflection from a surface. Modern ellipsometers use lasers, typically Helium-Neon lasers, as the source. The ellipsometer beam first goes through a polarizer so that only light orientated in a known direction is allowed to pass. It then goes through a device called a compensator, which elliptically polarizes the light beam. The remaining light is then bounced off the material under study.

The analysis is dependent on Snell's Law; when a beam of light strikes a material surface, some will reflect immediately, and some will pass through to the far side of the material before reflecting. By measuring the difference between the two reflections, the thickness of the film can be determined. The reflected light also undergoes a change in polarization; this change is used to calculate the refractive index and absorption coefficient.

For an ellipsometer to work properly, the material being examined must consist of more than one well-defined layer. The layers must be optically homogeneous,

have identical molecular structure in all directions, and have good reflection of light.

The ellipsometer used in this work is PLASMOS SD 2300 ellipsometer, manufactured by Philips (***Fig. 13***). The light source of the ellipsometer is a He–Ne laser with a wavelength of 632.8 nm.

Fig. 13. *A Philips PLASMOS SD 2300 ellipsometer and the user interface.*

The refractive indices of the films were measured by a spectroscopic ellipsometer (***Fig. 14***). The system works using multiplex detection and a step scan analyzer to measure ellipsometric angles ψ and Δ for a broad range of wavelength. The obtained spectra of ψ and Δ are compared with simulation to calculate the film thickness and the optical parameters. The system has a Xenon lamp, connected by a fiber optic cable with a polarizer as a light source and a FT-IR spectroscope with a diode array as a detector.

Fig. 14. *A spectroscopic ellipsometer SE 805 and its user interface.*

4.3 Preparation of substrates before ALD

The fabrication of samples was carried out in the Class 1000 clean room, which provided a contamination-free environment. To get an obvious profile of TiO_2 uniformity on a sample, big size silicon wafers of 25cm diameter were chosen as substrates. Silicon wafers were packaged and kept clean in a plastic box before using and were taken out one by one with clean tweezers. A UV light was used to inspect the particles on the substrate surface. The surface of silicon wafers was cleaned by using a high pressure nitrogen gas gun to remove the particles from the surface. Each wafer was parallel cut into four pieces. Therefore, each sample was grown on 1/4 of a wafer. Then particle inspection was done again to avoid crumb contamination during the cutting.

4.4 Optimization of parameters

Liquid phase $TiCl_4$ and H_2O were kept in separate cylinders as precursors. The deposition process was done by repeated ALD cycles. Each cycle consisted of a $TiCl_4$ pulse, purge length, an H_2O pulse and another purge length. As discussed in Chapter 2.2, growth temperature, number of cycles, precursor pulse length and purge length are the parameters which can affect the quality of a TiO_2 film in ALD. In this work nitrogen was used as a precursor carrier and purging gas. Purge length was kept constant as 2 s, which was long enough to avoid the precursor overlapping and to purge away the by-products produced by the reactions. The other parameters, growth temperature, number of cycles and precursor pulse length, were changed for optimization. ***Table 2*** lists detailed constant parameters in the process.

Growth temperature was changed from 100 °C to 450 °C manually by changing the reactor chamber temperature.

Table 2. *Experimental conditions for ALD growth of TiO_2.*

Used precursors	$TiCl_4$, H_2O
Precursor carrier and purging gas	N_2
$TiCl_4$ temperature (°C)	20
H_2O temperature (°C)	20
Precursor pulse length (H_2O) (ms)	250
Reactor pressure (mbar)	1
Chamber pressure (mbar)	8
Precursor pressure (mbar)	5
Precursor carrier and purging gas flow rate (sccm)	200

In the optimization of the pulse length other parameters were kept constant while the pulse length was varied from 100 ms to 600 ms. The pulse length at which the TiO_2 film had the best uniformity was used for the optimization of the temperature.

Chapter 5

Results and discussion

Samples were photographed in natural light (***Fig. 15***). Each sample represents different color at different temperature. The samples grown at 100 °C, 400 °C and 450 °C are shown in blue while the samples grown in the range of 200 °C – 350 °C are shown in brown.

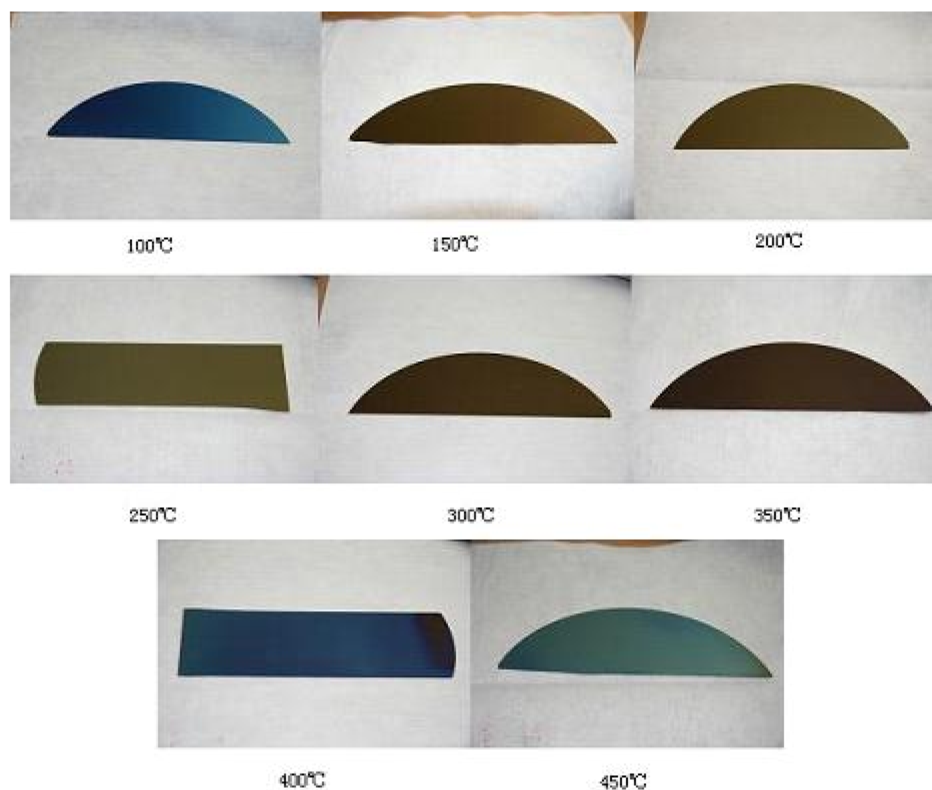

Fig. 15. *Photographs of samples of TiO_2 films at different temperatures.*

Films grown below 200 °C show a uniform surface while remarkable roughness can be observed on some of the films grown above 400 °C.

There may be two reasons for the color variation in different samples. One is probably the TiO_2 film thickness difference. The other reason is that different polymorphs may be formed at different temperatures. In general TiO_2 exhibits three polymorphs: rutile, anatase, and brookite.[39,40,41] The different crystal structures and refractive indices of the three polymorphs of TiO_2 result in different colors.

5.1 $TiCl_4$ pulse length optimization

In the $TiCl_4$ pulse length optimization experiment, the reactant sources were circularly injected into the reaction chamber in the following order: $TiCl_4$ vapor pulse, N_2 gas purge 2 s, H_2O gas pulse 250 ms and N_2 gas purge 2 s. $TiCl_4$ pulse lengths of 100 ms, 300 ms and 600 ms were used at different temperatures from 100 °C to 400 °C, respectively. 800 growth cycles were processed.

Fig. 16 indicates the dependence of the film thickness on the $TiCl_4$ pulse length at different temperatures. With exception of the samples grown at 100 °C, the thickness of the TiO_2 film does not depend linearly on the pulse length. For the samples grown in the range of 200 °C to 400 °C, a slight increase at 300 ms pulse length followed by a slight decrease at 600 ms pulse length is observed. The slight increase can be explained by the fact that the thickness can be enhanced by increasing the $TiCl_4$ dose, which is due to an increased density of titanium ligands remaining on the film surface after the $TiCl_4$ pulse. The slight decrease can be explained by an etching effect of the films. This behavior indicates that the

optimized self-limiting ALD reaction is reached at 100 ms pulse length.

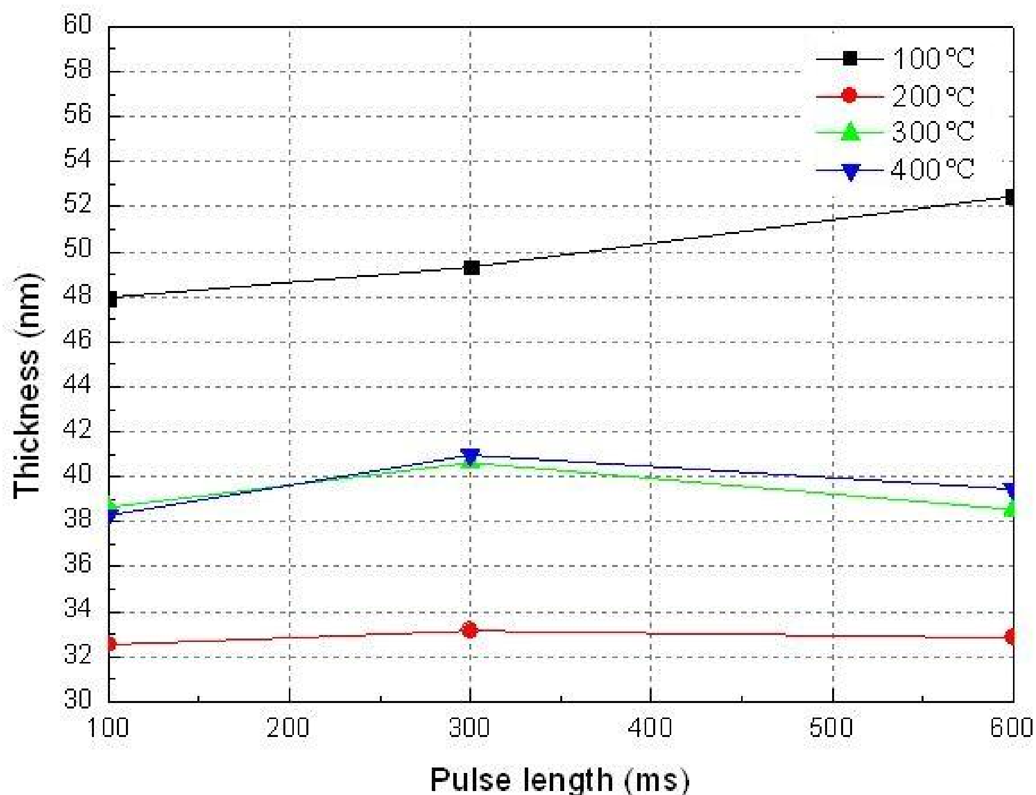

Fig. 16. *Thickness versus $TiCl_4$ pulse length at different temperatures.*

The mean thickness of the three films grown at the same temperature and the number of cycles was calculated as comparison***. Fig. 17*** indicates the thickness variation caused by different $TiCl_4$ pulse lengths at different temperatures. Longer pulse length resulted in great thickness variation at 100 °C, which indicates the precursor unsaturation.

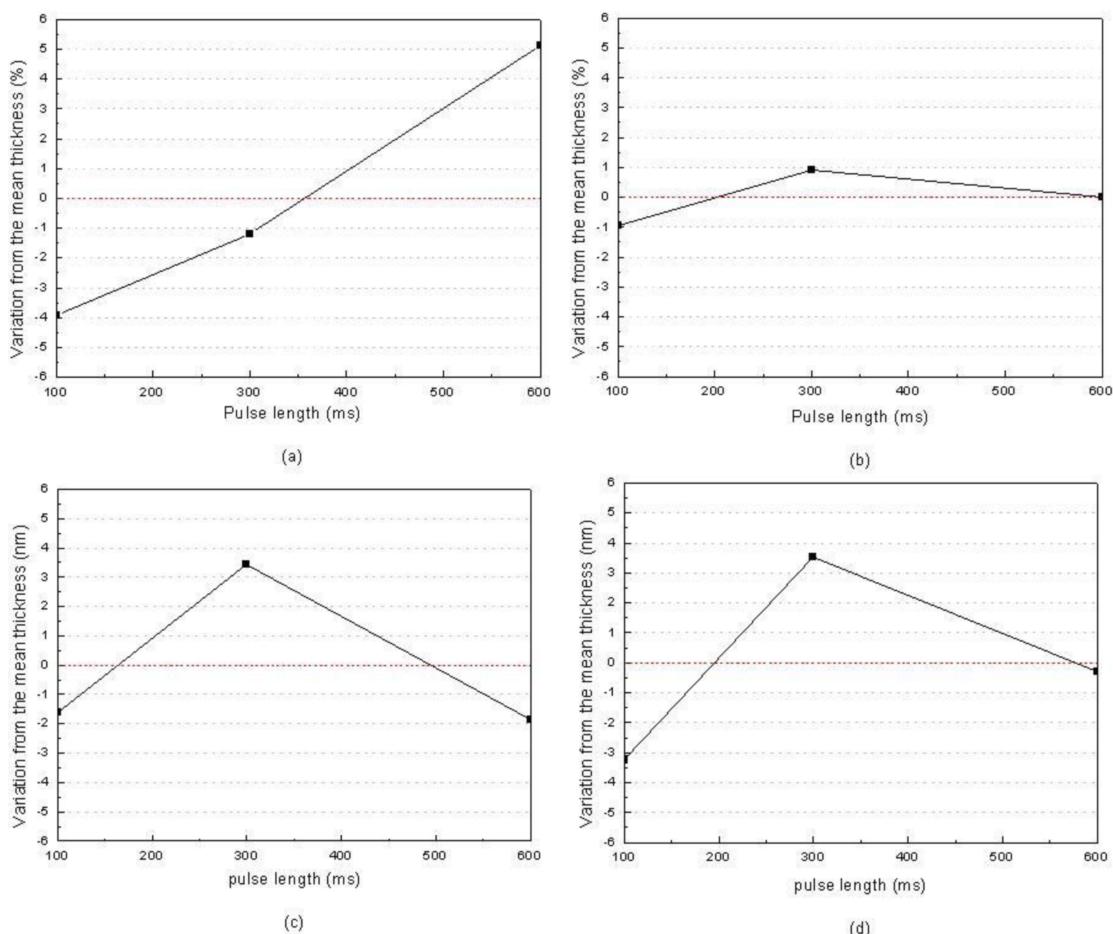

Fig. 17. *Variation of thickness compared to the mean thickness as a function of $TiCl_4$ pulse length. (a) 100 °C; (b) 200 °C; (c) 300 °C and (d) 400 °C.*

The changes of growth rate per cycle at different pulse lengths at different temperatures are shown in ***Fig 18***. The growth rate is almost at the same level of 0.4 Å/cycle at 200 °C and 0.48 Å/cycle at 300 °C to 400 °C, which is comparable to the result under different experimental conditions.[42] In an optimized self-limiting ALD process a constant growth rate per cycle is achieved despite lengthening the precursor exposures. Therefore, the self-limiting ALD process can be identified by the measurements of film thickness and growth rate against the $TiCl_4$ pulse length at 100 ms above 200 °C.

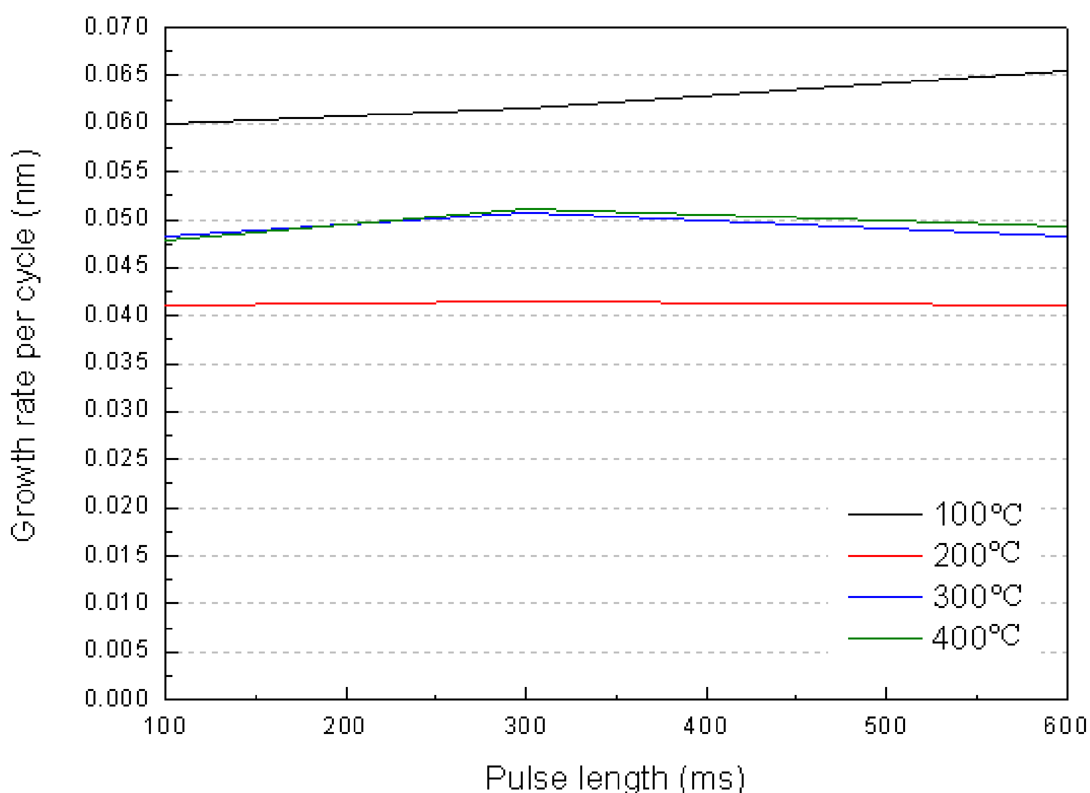

Fig. 18. *Growth rate per cycle versus pulse length at different temperatures.*

It is indicated that the growth rate increases with increasing TiO_2 dose at 100 °C. At 100 °C the saturation is not complete and occurs at significantly higher growth rates and precursor doses than at 200 °C to 400 °C. This demonstrates that the surface concentration of adsorption sites for precursor molecules depends on the temperature. A possible reason for such a dependence is the influence of temperature on the abundance of surface hydroxyl groups. At 100 °C a larger amount of –OH groups exist on the surface than at higher temperature.[43] It is known that metal chlorides are generally more reactive towards surface –OH groups than towards oxygen bridges. Thus more reaction sites provided by –OH groups result in the unsaturation of the precursor dose. Consequently the growth rate at 100 °C increases with a higher precursor dose.

However the influence of –OH group concentration does not play an important

role in the growth at 200 °C to 400 °C. Longer pulse length has no effect on the growth rate at 200 °C, while it results in an acceptable slight variation (about 0.05 Å/cycle) on the growth rate at 300 °C and 400 °C. The slight variation of growth rate with longer pulse length at 300 °C and 400 °C can be explained by the chlorine effect (see Chapter 2). An over dosing of $TiCl_4$ can result in more HCl and Cl^- occupying the adsorption sites, which hinders the adsorption of $TiCl_4$ and reduces the growth rate.

The uniformities of the films of 800 cycles are listed in ***Table 3***. The $TiCl_4$ pulse length resulting in the slightest variation at the same temperature is chosen for the following ALD growth. Thus 100 ms, 600 ms, 300 ms and 600 ms were chosen for the following ALD growth at the temperature of 100 °C, 200 °C, 300 °C and 400 °C, respectively.

Table 3. *Selection of $TiCl_4$ pulse length depending on thickness variation.*

Temperature (°C)	$TiCl_4$ pulse length (ms)	Uniformity (%)
100	100	1.58
100	300	1.95
100	600	8.87
200	100	1.30
200	300	4.73
200	600	1.17
300	100	5.69
300	300	5.16
300	600	7.16
400	100	5.86
400	300	8.74
400	600	4.25

Table 3 indicates that a longer pulse length of $TiCl_4$ increases the thickness variation at all temperatures. This can be explained by the chlorine effect also. More HCl released after the over dosing of $TiCl_4$ may react with the surface. The by-product and residues produced by the reaction may have an effect on the structural arrangement of atoms on the surface, resulting in the poor uniformity. At 100 °C the large –OH group provides an interactive reaction environment between the precursors and by-products. Complicated surface reactions give rise to the bad uniformity.

On the other hand, a longer pulse length and too short purge length can result in precursor residue and desorption of the precursor at the beginning of the next pulse. Hence CVD-type growth occurs and results in bad uniformity owing to the mixing of the precursors.

5.2 Growth linearity

In order to investigate growth linearity, another set of TiO_2 films with different cycles were grown at different temperatures with the optimized $TiCl_4$ pulse length while keeping the other parameters constant. 200, 500 and 800 cycles were processed.

5.2.1 Thickness and growth linearity

Fig. 19 shows the thickness dependence on the number of cycles at different temperatures. In perfect ALD growth the thickness dependence on the number of cycles is expected to be a linear curve starting from the origin of coordinates.

However, if a whole curve simulation across the origin of coordinate is made on the basis of the figure, the curve is not linear. The thickness shows a rapid increase in the initial cycles at 100 °C.

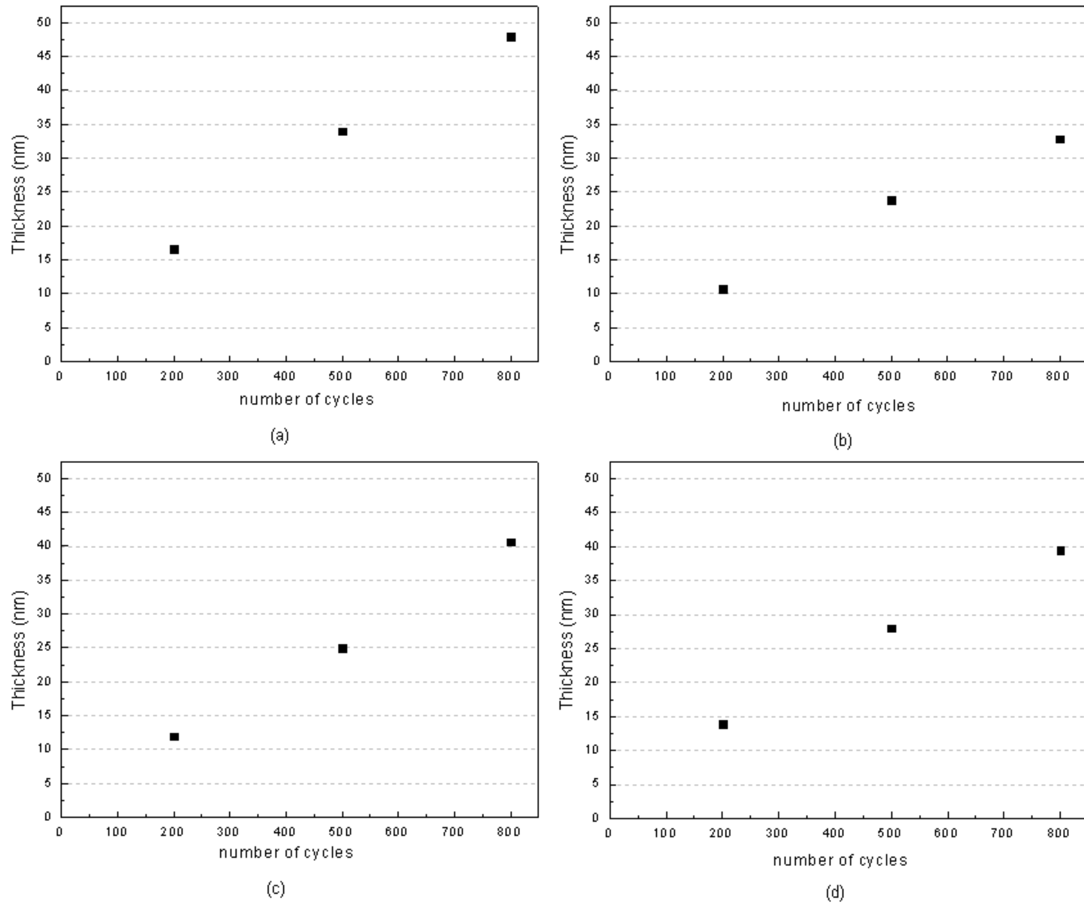

Fig. 19. *Thickness versus number of cycles at (a) 100 °C; (b) 200 °C; (c) 300 °C and (d) 400 °C.*

5.2.2 Growth rate versus number of cycles

The growth rate per cycle in 200, 500 and 800 cycles at 100 °C, 200 °C, 300 °C and 400 °C is presented in ***Fig. 20***.

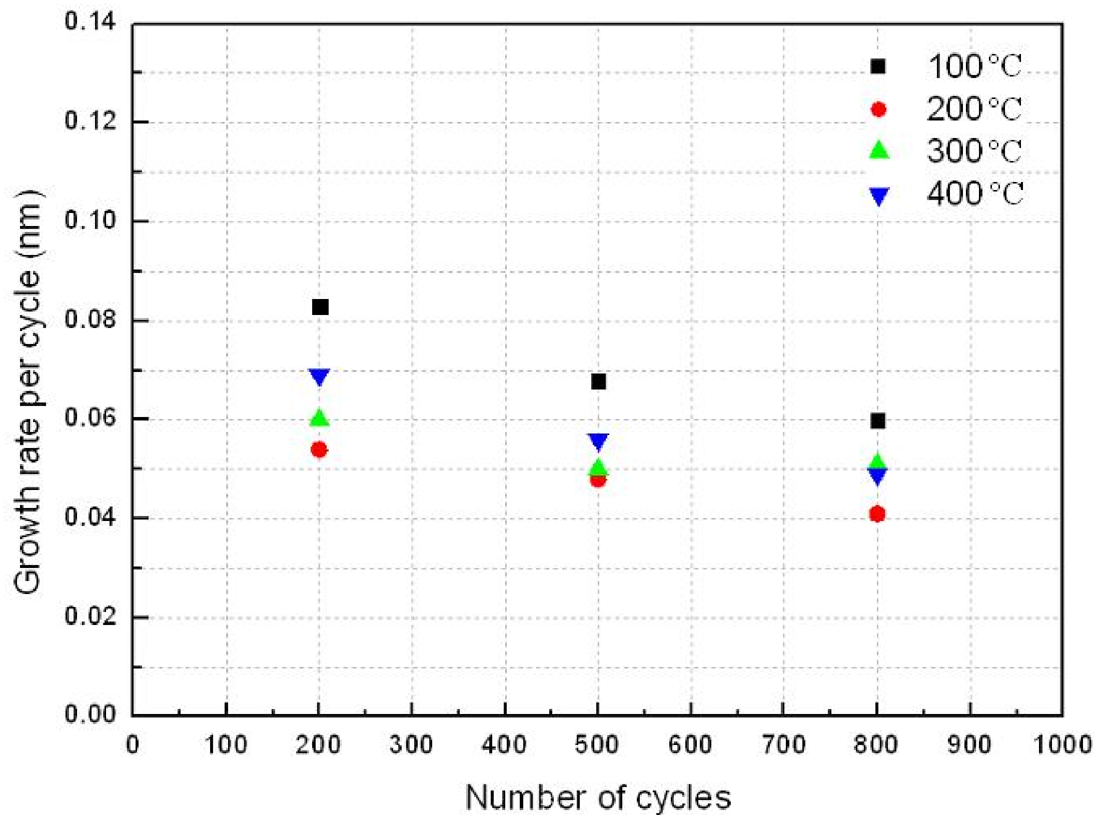

Fig. 20. *Growth rate versus number of cycles at different temperatures.*

The growth rate per cycle decreases with a moderate gradient as the number of cycles increases. The reason for such substrate-enhanced growth (see chapter 2.2.2.) may be that on a TiO_2-grown material the number of reactive sites is lower than on a bare substrate. At the temperature of 300 °C, the growth rate per cycle settled to a constant as in an ideal ALD growth mode.

5.3 Optimization of temperature

In the temperature optimization experiment, the reaction chamber temperature was changed as 100 °C, 200 °C, 300 °C, and 400 °C. An optimized pulse length was applied as 100 ms, 600 ms, 300 ms and 600 ms, respectively, based on the

previous experiments while the other parameters were kept the same. 800 cycles were applied. The optimization is based on the assumption that no temperature variation exists on the substrate in each process.

5.3.1 Temperature dependence of growth rate

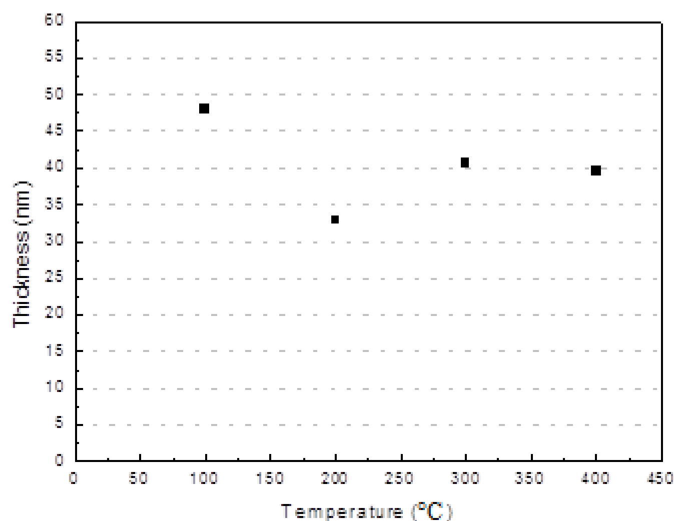

Fig. 21. *Thickness of the TiO_2 films versus temperature.*

An obvious variation of the TiO_2 film thickness between 33 nm and 49 nm was observed as illustrated in ***Fig. 21***. At 100 °C steric hindrance of chloride does not define saturation owing to a small Cl/Ti ratio. The reason for reduced chloride concentration in the surface intermediate species formed at temperatures below 200 °C is the evidently increasing abundance of hydroxyl groups or even molecular water on the surface where $TiCl_4$ is adsorbed. At temperatures above 200 °C, however, a larger Cl/Ti ratio in the adsorbate layer is connected with a decreasing number of hydroxyl groups. Thus steric hindrance seems to define saturation. At temperatures above 300 °C, the effect of surface microstructure on the TiO_2 growth is more significantly related to the number of adsorption sites

than to the changes in adsorption and/or mechanisms. A probable reason for the increased number of adsorption sites on the surface of films grown at above 300 °C is faster decomposition and agglomeration of the surface intermediate species and corresponding increase in the effective surface area.[44]

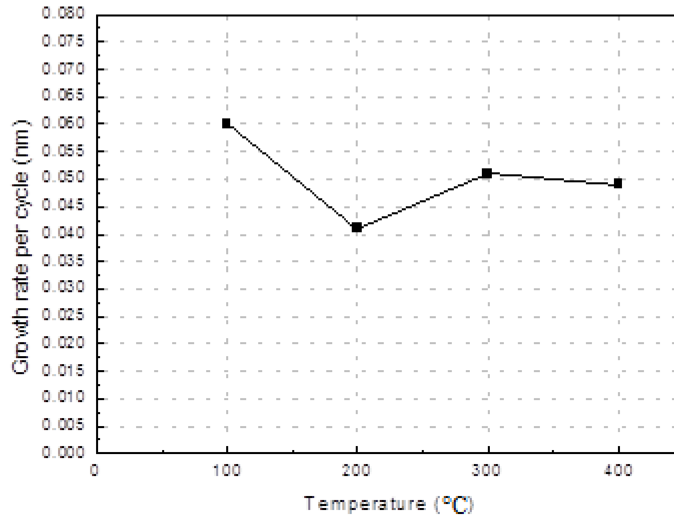

Fig. 22. *GPC of the TiO_2 films versus temperature.*

Fig. 22 shows that the growth rate per cycle remains constant (0.4 Å - 0.5 Å per cycle) from 200 °C to 400 °C. It indicates that the temperature range of 200 °C to 400 °C is within the acceptable ALD growth window. The growth rate at 100 °C is remarkably increased compared to those at 200 °C to 400 °C. This seems to be related to the concentration of surface –OH groups. The concentration of surface –OH groups is higher at low temperature, which leads to a large number of active sites, resulting in a higher growth rate at low temperature.[45] Similar results have been reported in other articles.[46, 47]

5.3.2 Temperature dependence of uniformity

For the purpose of investigating the temperature effect on film roughness, a clear thickness profile of the samples along the flow direction at 100 °C, 200 °C, 300 °C and 400 °C was sketched (***Fig. 23***). Thickness at 20 points along the flow direction on each sample was measured. All the films represent a relative smooth surface.

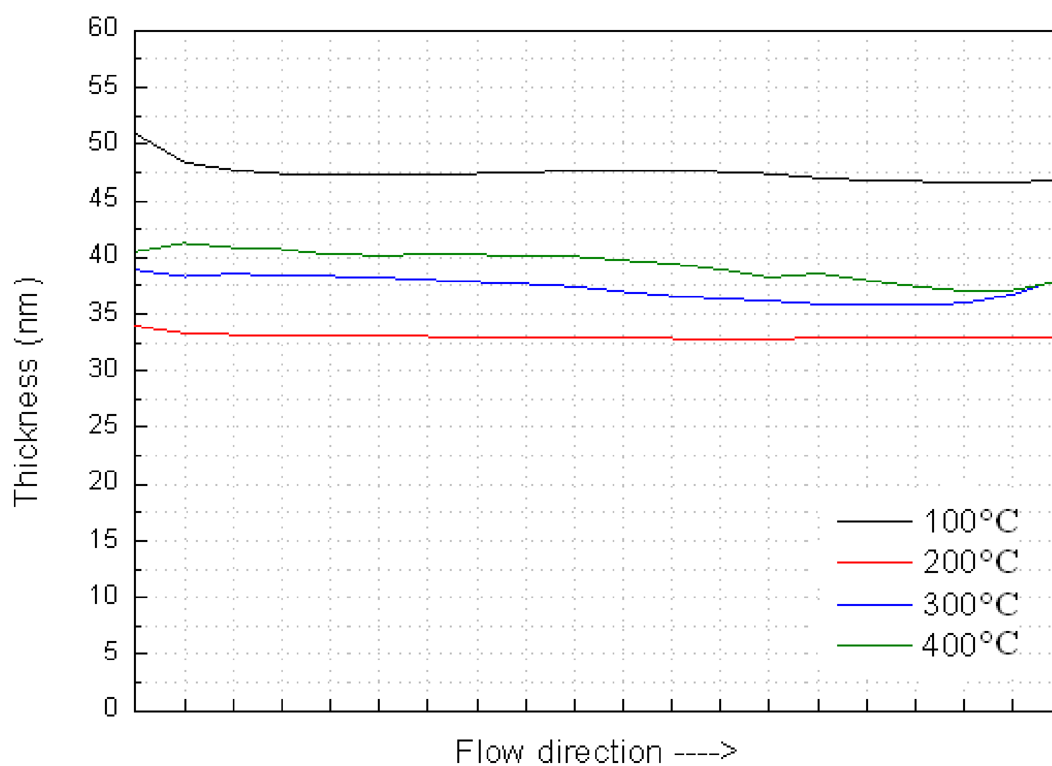

Fig. 23. *Thickness profiles of samples grown at different temperatures.*

Fig. 24 shows the thickness variation profile of films of 800 cycles grown at different temperatures. The thickness of the flow-leading position is higher than that of the trailing position for almost all the samples. It can be explained by the different precursor densities between the flowing-leading position and the trailing position in the reaction chamber. When the $TiCl_4$ pulse propagates along a flow

channel, the hydroxyl groups are effectively consumed in reactions with $TiCl_4$ at the $TiCl_4$ pulse front. The reaction by-product, HCl, travels in front of the $TiCl_4$ pulse and may readsorb at trailing position and block the reaction sites from $TiCl_4$. Thus the $TiCl_4$ density adsorbed at the flow-leading position is higher than that at the trailing position along the flow direction, which can result in a more saturated reaction.

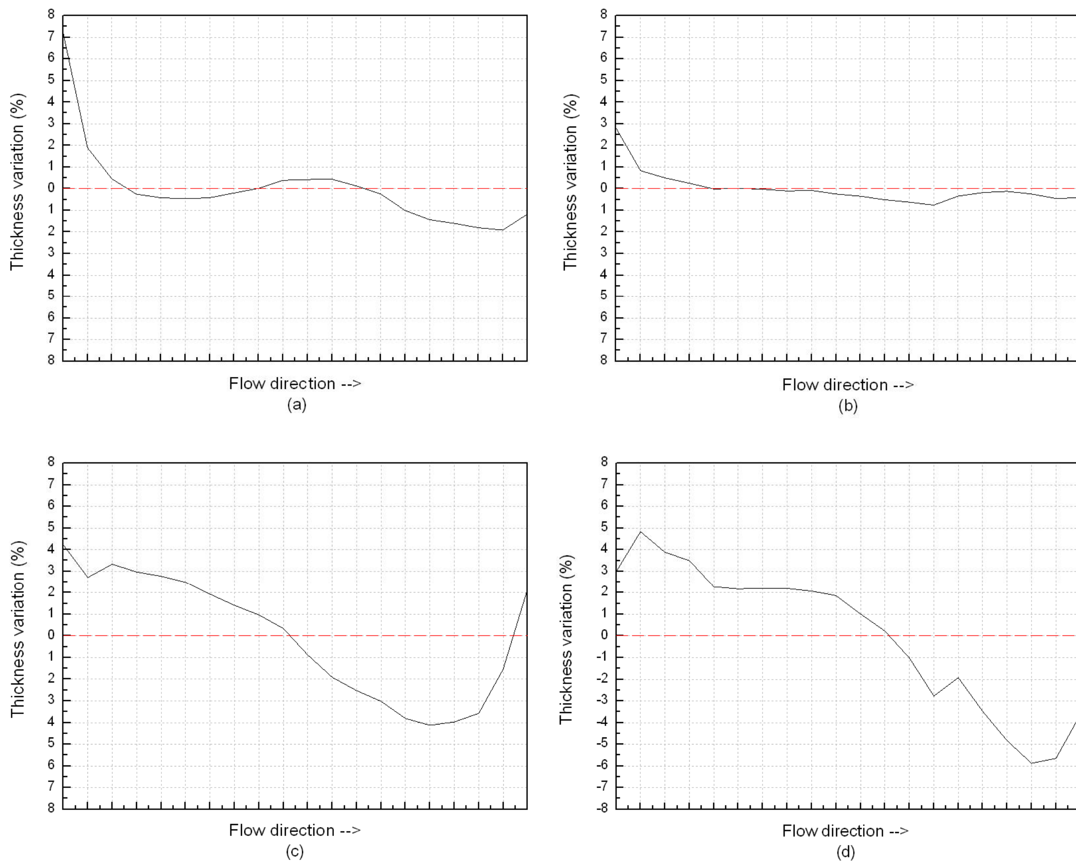

Fig. 24. *Thickness variation profile at (a) 100 °C, (b) 200 °C, (c) 300 °C and (d) 400 °C.*

At the temperature of 300 °C and 400 °C, the first half located next to the leading edge of the substrate is characterized by a steep thickness profile. Thickness decrease was observed at the flow-leading position owing to the active reaction of by-product residues at high temperature. Etching reaction by the corrosive

chlorine on the ALD-grown surface before purging resulted in the reduction of the amount of TiO_2.

At the temperature of 100 °C, the leading edge part of the substrate is characterized by an exceptional sharp thickness variation despite the relatively good uniformity of the latter part. This sharp increase of the thickness at the edge can be explained by the CVD reaction at the edge owing to the water formation. A large amount of –OH groups result in a high concentration of water at the edge (***E.q. 3.4, E.q. 3.5***). If the water formation occurs during the $TiCl_4$ pulse, a CVD-type growth may take place.

Fig. 25 shows the uniformity of 500-cycle and 800-cycle TiO_2 films as a function of temperature processed in. It can be seen that a larger number of cycles can contribute to a more favorable uniformity. This is reasonable since in the initial stage of the surface reaction, film formation may be low in density or even porous, while more cycles can compensate the crystal arrangement.

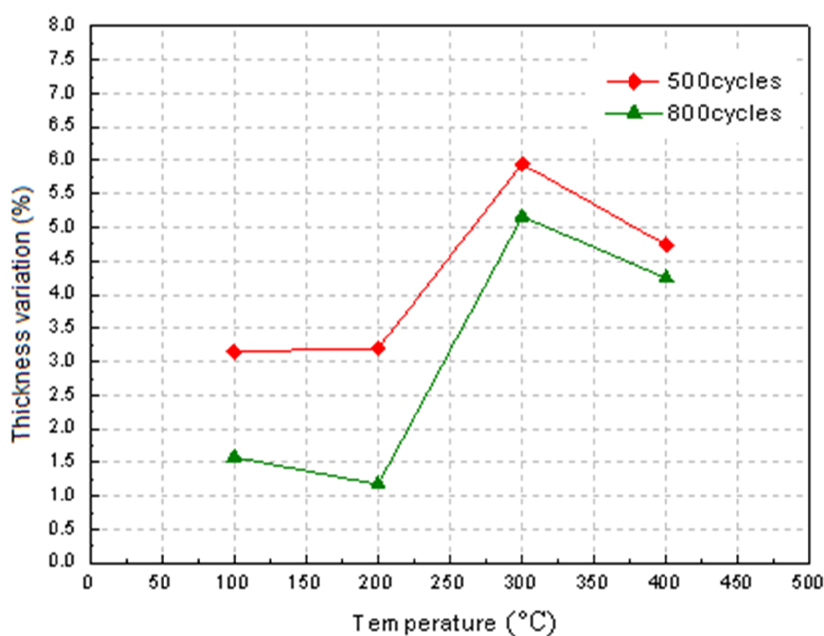

Fig. 25. *Uniformity of the TiO_2 films versus temperature at different cycles.*

Among the films of 800 cycles gown at 100 °C, a favorable uniformity can be obtained (thickness variation of 1.5%) with an appropriate $TiCl_4$ pulse length (100 ms), while the thickness variation can rise up to 8% with a longer pulse length. At 200 °C more flat films can be produced with the thickness variation of 1.5% - 4%. In the temperature range of 300 °C to 400 °C, the thickness variation of the films rises up to a range of 5% - 8%. Heterogeneous composition of the surface reaction ligands and by-products on the surface at different temperatures could be the main reason.

On the one hand, concentration of –OH groups should be taken into consideration. As mentioned before, the amount of –OH groups on the reaction surface are different depending on temperature. The quantity of –OH groups are largely increased and they are more reactive at low temperature (100 °C or even lower) than at high temperature, resulting in much more reactive sites on the surface. At 100 °C the growth is unsaturated and CVD-type growth may occur owing to the gas phase H_2O formation, which degrades the uniformity of the film. At high temperature above 400 °C, decrease of reaction sites provided by –OH groups leads to weak and inhomogeneous chemisorption of precursors and re-evaporation of the precursors on the surface. Consequently, the uniformity is significantly affected.

On the other hand, the interaction between the by-products and the surface is more reactive when metal halide and water are used as precursors. A strong assumption is provided that the non-uniformity is mainly caused by the hydrochloride by-product.[48] At high temperature above 300 °C, etching reaction by hydrochloride occurs and the possible reaction product, oxychloride, can be a source of surface contaminations.

In addition, $TiCl_4$ slightly decomposes at high temperatures. Growth mechanism becomes complicated because of the structural change of the oxide,[49] which has an effect on the uniformity at high temperatures.

5.4 Optical characterization of TiO_2 films

The results of the refractive indices of the films measured by spectroscopic ellipsometry are presented in ***Fig. 26***. The wavelength range of the incident light was 800 nm to 1600 nm and the incident angle was changed from 45° to 75°.

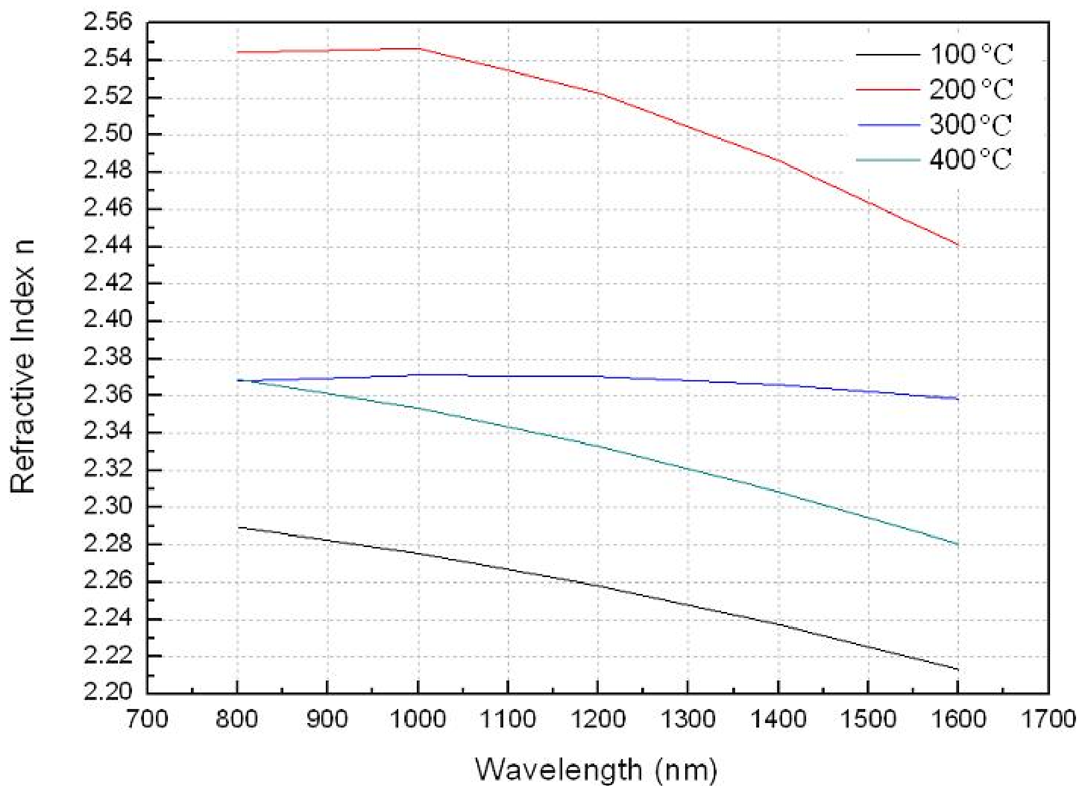

Fig. 26. *Refractive index versus wavelength at different temperature: (a) 100 °C, (b) 200 °C, (c) 300 °C and (d) 400 °C.*

Films grown at different temperatures have different refractive indices. This can

be explained by the different crystal structures formed at different growth temperatures. J. Aarik et al. reported that films grown below 165 °C were amorphous while those deposited at 165 °C - 350 °C contained the anatase phase. At 350 °C - 500 °C rutile was the most dominating phase.[50] The refractive index of an anatase crystallize TiO_2 film is usually 2.5 while a rutile crystallize one can have a refractive index of 2.9.[51] In this work the refractive indices of the films grown at 200 °C and 300 °C were high, indicating a dense molecular concentration and a high film quality. The refractive index of the film grown at 200 °C has the value of above 2.54 at the wavelength of 800 nm, which is comparable to the result reported in the doctoral thesis of V. Pore.[52]

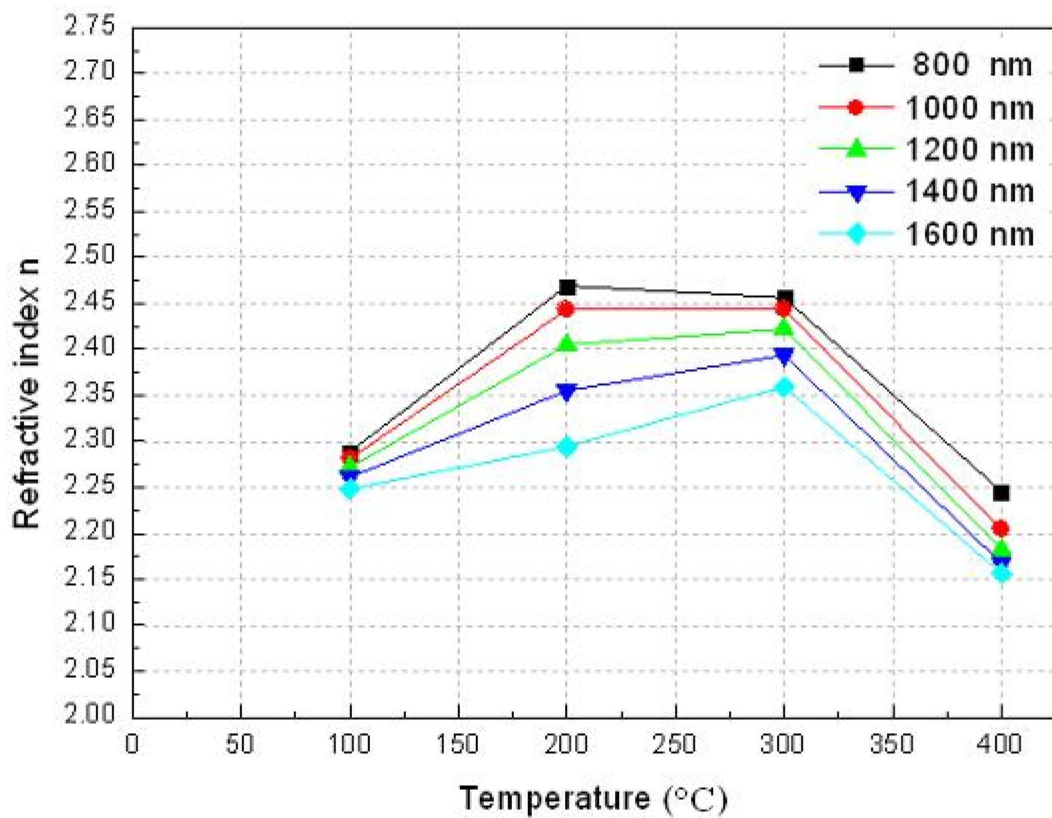

Fig. 27. *Refractive index versus temperature with different wavelengths used.*

The dependence of refractive indices at different temperatures is presented in ***Fig. 27***. At growth temperatures lower or higher than 200 °C to 300 °C the refractive indices were lower. The films grown at 300 °C and 400 °C have subequal thickness (about 40 nm) but represent quite different refractive indices, which are 2.45 and 2.2 at the wavelength of 1000 nm, respectively. The different surface morphology is a reliable explanation to the refractive indices difference.

Another assumption for the reason of low refractive index is that low density or even porous films were produced at 100 °C. Owing to the fact that the film grown at 100 °C has the highest thickness compared to those grown at 200 °C to 400 °C but a low refractive index, it might be presumed that the low value of the refractive index of the films grown at 100 °C is related to residual chlorine. Surface impurities result in a lower atomic concentration of TiO_2 of the film. On the other hand, high refractive indices represent the smoothness of the films grown at 200 °C and 300 °C.

Chapter 6

Conclusions

ALD technique offers better thickness control and uniformity than other deposition techniques. In ideal case the uniformity of a film grown by ALD should be excellent, but in real fabrication some external factors, like growth temperature, number of cycles, precursor pulse length and purge length may affect ALD growth. In this work, relationship among growth temperature, precursor pulse length, growth rate, uniformity, refractive index and crystallinity of TiO_2 thin films were investigated. The investigation helps to have an understanding of the precursor pulsing effect and the temperature dependence on ALD growth.

The result of the pulse length optimization shows that precursor dose is one of the parameters which can affect film growth rate and uniformity. The effect of pulse length is concerned with growth temperature. At temperatures above 200 °C the growth rate is independent of the pulse length while it increases with increasing pulse length at lower temperature. Over dose of TiO_2 can result in non-uniformity due to the chlorine effect.

The result of the temperature optimization indicated that ALD growth is temperature sensitive. The ALD window of TiO_2 is in the temperature range of 200 °C to 300 °C in which temperature changes cause relatively slight changes to

the growth rate. A film thickness decrease in the direction of gas flow was observed, which was attributed to by-product residues.

It can be concluded that the best uniformity can be obtained at the temperature of around 200 °C and 300 °C. Film thickness in this temperature range is moderate with comparatively excellent uniformity and high refractive index. It can be concluded that 300 °C is an applicable temperature for TiO_2 film growth resulting in saturated surface reactions. The reason may be that at around 300 °C precursors are the most reactive without decomposition or etching reactions. However, deviations from the self-limiting growth mode appear at the deposition temperatures of 100 °C and lower. Moreover, the film density and refractive index decrease with decreasing growth temperature.

In the future, work should be concentrated on the improvement of film uniformity by for example temperature gradient control over the substrate to compensate the roughness caused by the by-products. The work should also involve optimization of other novel material film growth such as ALD of metal fluorides.

REFERENCES

[1] H. K. Pulker, *Thin Film Science and Technology, Vol. 6, Coatings on Glass*, Elsevier, Amsterdam, 1984.

[2] J. M. Bennett, E. Pelletier, G. Albrand, J. P. Borgogno, B. Lazarides, C. K. Carniglia, R. A. Schmell, T. H. Allen, T. T. Hart, K. H. Guenther, A. Saxer, *Appl. Opt.* 28, 3303, 1989.

[3] A. Fujishima, K. Hashimoto, T. Watanabe, *TiO_2 Photocatalysis, Fundamentals and Applications*, BKC Inc., Tokyo, 1999.

[4] A. Mills, S. K. Lee, *J. Photochem. and Photobiol*. A 152, 233, 2002.

[5] J. Wu, S. Hayakawa, K. Tsuru, A. Osaka, *Thin Solid Films* 414, 283, 2002.

[6] R. Matero, M, Ritala, M. Leskelä, T. Salo, J. Aromaa, O. Forsen, *J. Phys. IV* 9, Pr8-493, 1999.

[7] S. A. Campbell, H. S. Kim, D. C. Gilmer, B. He, T. Ma, W. L. Gladfelter, *IBM J. Res. and Dev.* 43, 383,1999.

[8] M. Grätzel, *Comments Inorg. Chem*. 12, 93, 1991.

[9] L. C. Klein, *Sol-gel technology for thin films, fibers, preforms, electronics, and specialty shapes*, ISBN: 0-8155-1154-X, 1988.

[10] L. M. Williams and D. W. Hess, *J. Vac. Sci. Technol. A* 1, 1810, 1983.

[11] G. A. Battiston, R. Gerbasi, M. Porchia and A. Marigo, *Thin Solid Films* 239, 186, 1994.

[12] K. Narasimha Rao, M. A. Murthy and S. Mohan, *Thin Solid Films* 176, 181, 1989.

[13] H. Tang, K. Prasad, R. Sanjines, P. E. Schmid and F. Levy, *J. Appl. Phys*. 75, 2042, 1994.

[14] S. Ben Amor, G. Baud, J. P. Besse and M. Jacqet, *Thin Solid Films* 293, 163, 1997.

[15] M. Gilo and N. Croitoru, *Thin Solid Films* 283, 84, 1996.

[16] M. Ritala and M. Leskela, in: H. S. Nalwa, (Ed), *Handbook of Thin Film Materials*, *Academic Press, San Diego*, Vol. 1, Chap. 2, 103-159, 2002.

[17] R. L. Puurunen, *J. Appl. Phys*. 97, 1213011, 2005.

[18] GCEP project research webpage, Standford University, 2005.

[19] T. S. Suntola, A. J. Pakkala, and S. G. Lindfors, US Patent 4 413 022, 1983.

[20] L. Niinistö, M. Leskelä, *Thin Solid Films* 225, 130, 1993.

[21] R. L. Puurunen, S. M. K. Airaksinen, and A. O. I. Krause, *J. Catal*. 213, 281, 2003.

[22] L. Niinistö, J. Päiväsaari, J. Niinistö, M. Putkonen, M. Nieminen, *Phys. Stat. Sol. (a)* 201, No. 7, 1443-1452, 2004.

[23] J. S. Becker, S. Suh, S. Wang, and R. G. Gordon, *Chem. Mater*. 15, 2969, 2003.

[24] J. Ihanus, E. Lambers, P. H. Holloway, M. Ritala and M. M. Leskelä, *J. Cryst. Growth* 260, 440, 2004.

[25] R. L. Puurunen and W. Vandervorst, *J. Appl. Phys.* 96, 7686, 2004.

[26] M. Ritala, M. Leskelä, L. Niinisto and P. Haussalo, *Chem. Mater.* 5, 1174, 1993.

[27] J. Aarik, A. Aidla, T. Uustare, M. Ritala and M. Leskelä, *Appl. Surf. Sci.* 161, 385, 2000.

[28] V. Pore, A. Rahtu, M. Leskelä, M. Ritala, T. Sajavaara and J. Keinonen, *Chem. Vap. Deposition* 10, 143, 2004.

[29] G. T. Lim and D. H. Kim, *Thin Solid Films* 498, 254, 2006.

[30] R. L. Puurunen, *Chem. Vap. Deposition* 9, 327, 2003.

[31] H. Fujiwara, *Spectroscopic ellipsometry: principles and applications*. John Wiley & Sons, Ltd., 2007.

---

[32] An image from en.wikipedia.org/wiki/polarization.

[33] R. M. A. Azzam, *Opt. Lett.* 34, 3, 2009.

[34] R. L. Puurunen, *J. Appl. Phys*. 97, 1213011, 2005.

[35] An image from www.dowcorning.com.

[36] Thin Film System TFS 500 user manual, BENEQ Oy.

[37] An image from BENEQ Oy website www.beneq.com.

[38] D. Gonçalves and E. A. Irene, *Fundamentals and applications of spectroscopic ellipsometry*. Quím. Nova Vol. 25, No. 5, São Paulo Sept./Oct., 2002.

[39] X. Z. Ding, X. H. Liu, Y. Z. He, *J. Mater. Sci. Lett.* 15, 1789, 1996.

[40] J. Jamieson, B. Olinger, *Mineralog. Notes* 54, 1477, 1969.

[41] S. J. Smith, R. Stevens, S. Liu, G. Li, A. Navrotsky, J. Boerio-Goates, B. F. Woodfield, *Am. Miner.* 94, 236, 2009.

[42] J. D. Fergusona, A. R. Yoderb, A. W. Weimerb, S. M. George, *Appl. Surf. Sci.* 226, 393-404, 2004.

[43] S. Haukka, E. L. Lakomaa and A. Root, *J. Phys. Chem*. 97, 5085-5094, 1993.

[44] J. Aarik, A. Aidla, H. Mändar and T. Uustare, *Appl. Surf. Sci.* 172, 148-158, 2001.

[45] J. Aarik, A. Aidla, V. Sammelselg, H. Siimon and T. Uustare, *J. Cryst. Growth* 169, 496, 1996.

[46] T. Nam, J. M. Kim, M. K. Kim and H. Kim, *J. Korean Phys. Soc.* 59, 452-457, 2011.

[47] Q. Xie, Y. L. Jiang, C. Detavernier, D. Deduytsche, R. L. V. Meirhaeghe, G. P. Ru, B. Z. Li and X. P. Qu, *J. Appl. Phys*. 102, 083521, 2007.

[48] K. E. Elers, T. Blomberg, M. Peussa, B. Aitchison, S. Haukka, and S. Marcus, *Chem. Vap. Deposition* 12, 13-24, 2006.

[49] K. Kukli, A. Aidla, J. Aarik, et al., *Langmuir* 16, 8122, 2000.

[50] J. Aarik, A. Aidla, T. Uustare and V. Sammelselg, *J. Cryst. Growth* 148, 268, 1995.

[51] U. Diebold**,** *Surf. Sci. Rep.,* 48, 53-229, 2003.

[52] V. Pore, Academic Dissertation, ISBN 978-952-92-7359-1, Helsinki University, 2010.